

Article

Stochastic Model Predictive Control Based Scheduling Optimization of Multi-Energy System Considering Hybrid CHPs and EVs

Xiaogang Guo, Zhejing Bao * and Wenjun Yan

College of Electrical Engineering, Zhejiang University, Hangzhou 310027, China;
guoxiaogang@zju.edu.cn (X.G.); yanwenjun@zju.edu.cn (W.Y.)

* Correspondence: zjba@zju.edu.cn; Tel.: +86-571-8795-3959

Received: 10 December 2018; Accepted: 13 January 2019; Published: 21 January 2019



Abstract: Recently, the increasing integration of electric vehicles (EVs) has drawn great interest due to its flexible utilization; moreover, environmental concerns have caused an increase in the application of combined heat and power (CHP) units in multi-energy systems (MES). This paper develops an approach to coordinated scheduling of MES considering CHPs, uncertain EVs and battery degradation based on model predictive control (MPC), aimed at achieving the most economic energy scheduling. After exploiting the pattern of the drivers' commuting behavior, the stochastic characteristics of available charging/discharging electric power of aggregated EVs in office or residential buildings are analyzed and represented by the scenarios with the help of scenario generation and reduction techniques. At each step of MPC optimization, the solution of a finite-horizon optimal control is achieved in which a suitable number of available EVs scenarios is considered, while the economic objective and operational constraints are included. The simulation results obtained are encouraging and indicate both the feasibility and the effectiveness of the proposed approach.

Keywords: combined heat and power (CHP); electric vehicles (EVs); model predictive control (MPC); multi-energy system (MES); optimization; stochastic

1. Introduction

Nowadays, great concerns about energy crisis and environment problems are encouraging more efficient energy management and consumption. Residential and commercial buildings consume about 32% of the global energy use, in which usually there are multi-energy demands, such as electricity and heat [1]. It is particularly important to change the existing energy systems which are individually designed to operate separately, and to build various energy systems as an integrated whole in order to improve the overall energy utilization efficiency and lower environmental pollution. Therefore, some coupled energy systems, such as the multiple-energy carriers system (MCES) [2] and the multi-energy system (MES) [3], have been investigated in recent years. The essential characteristics of these systems is the interaction of diverse forms of energy, such as heat power, electrical power, nature gas, renewable energies and so on. However, the uncertainty and randomness of the MES considering electric vehicles (EVs) and renewable energy are still a challenge for scheduling optimization in MES.

The integration of EVs and combined heat and power (CHP) units have an increasing impact on the distribution grid and will change the buildings' electricity consumption and supply. In general, EVs are parked for more than 90% of the time and EVs charging/discharging flexibility can be utilized fully, although the charging/discharging is limited by battery limitations, the mobility objectives,

the available power ratings and battery state of charge (SOC). Consequently, as one of the most important components in energy systems due to their advantages of flexible charging/discharging and zero emission, EVs can connect to the MES in the form of Grid-to-Vehicle (G2V) or Vehicle-to-Grid (V2G) [4]. However, on one hand, the electricity consumption of EVs in G2V mode may lead to peak loads, higher resistive losses, voltage deviations, and phase unbalance in the grid [5]; on the other hand, in contrast to other electrical equipment, the integration of EVs simultaneously connected in parking stations could be considered as a potential source for the demand respond in the MES. However, the uncertain arrival/departure time induced stochastic availability of aggregated EVs should be considered carefully. As a significant means to improve energy efficiency, CHP units have received increasing attention owing to their ability in providing electrical and thermal power simultaneously, but they have to remain on certain constrained electric power output to meet the heat loads' demand. Therefore, the scheduling coordination between the aggregated EVs and CHP units in MES is crucial to improve the system operational flexibility and enhance energy efficiency.

Extensive research has been conducted on the optimal operation of MES, which is modeled based on the integration of EVs, CHPs, or other renewable energies. Ref. [6] presented an approach to solve the CHP unit commitment problem in the presence of plug-in EVs as small portable generation units in addition to typical generation constraints. In Ref. [7], a multi-objective optimization algorithm was proposed for minimization of energy cost and emissions for residential microgrids considering combined cooling heating and power (CCHPs), electric and thermal energy storage and EVs. A two-stage stochastic programming was used to minimize the operational cost of a microgrid by using scenario generation and a reduction technique [8]. Ref. [9] investigated the optimization and energy management in smart homes considering photovoltaic, wind, and battery storage systems with integration of EVs through a heuristic technique. Ref. [10] provided a number of stochastic programming models for optimal decision-making under uncertainty in electricity markets and electric energy systems with a large integration of non-dispatchable sources. A closed-loop V2G control to achieve both the frequency regulation and the EV charging demands was studied by a hierarchical control structure considering the uncertain dispatch in Ref. [11]. In Ref. [12], an optimal energy management scheme to charge or discharge EVs efficiently was developed by considering vehicle-to-building (V2B), renewable energy source (RES) and energy storage system (ESS) considering driver behavior. A robust stochastic shortest path model to stochastically match the EV charging load with the wind supply was studied in Ref. [13]. Ref. [14] developed a multi-objective model for Multi-Energy Complementary System (MECS) operation considering different operation constraint conditions under three objective functions. Ref. [15] analyzed the unbalance of plug-in EVs home charging in distribution network by stochastic load model. In Ref. [16], an Eco-town based MES in UK was simulated to research the optimal size and operation strategy of mixed technologies such as fuel cell, CHP, gas boiler and PV to meet the electrical and thermal loads. Ref. [17] developed a method for scheduling EVs charging based on probabilistic models. The authors in [18] studied a stochastic model of the home energy management (HEM) considering the uncertainties of EVs availability and small-scale renewable energy generation, as well as the customers' satisfaction by developing a response fatigue measure. Ref. [19] proposed leveraging day-ahead power market and time-of-use electricity, and use stochastic programming to address the uncertainties in EV charging demand.

In the above literature on integrated electricity and the heat system, the operational optimization modelling of electricity and heat energy as a whole, considering various CHP units with complementary properties, is limited. It is well known that, in MES, the electricity demand is independent from heat demand; on the contrary, the electricity generation is coupled with heat production due to the constraints on operational characteristics of CHP units, which makes the coordinated optimization intractable under the constraints of multi-energy supply/demand balance. Consequently, how to coordinately schedule the multi-energy generation in MES with various CHPs, i.e., the fixed or variable heat-to-electricity ratio, is imperative. Moreover, on the uncertainties of EVs included in MES, some work used the deterministic modeling to

formulate the scheduling of MES, without further discussing the stochastic model of EV availability and driving pattern [7,9,11]; in other work, although the stochastics were considered, the coordination between electricity and thermal multi-energy was involved simply. As for the costs of EVs' batteries degradation, little research included it in the coupled scheduling optimization of multi-energy, which is important for realizing the high efficiency operation control for CHP units with the unmatched heating and electric power demands [12–19].

As the driver information and the stochastic model of EVs availability are not easily exploited by classical control strategies, model predictive control (MPC) appears to be suitable for this purpose. Recently, MPC has drawn the attention of the power system community and consequently the research to show the advantages of applying MPC to dynamic economic dispatch with the uncertainties considered have been implemented. Initially, the EVs and CHP power coordination is made for the MES in order to create a power balance between power generation and demand. Then, this method optimizes a control sequence over a receding horizon to predict the future system behavior [20]. MPC is based on iterative, finite-horizon optimization of the controlled model. In MPC, at each time step, the solution to the optimal control problem is solved over a certain pre-defined horizon using the current state of the system as the initial state. The optimization calculates a control sequence for the whole horizon such that the selected objectives are minimized, but only the control action for the next time step is implemented in the system [21]. In Ref. [20], the authors develop an approach for driver-aware vehicle control based on stochastic model predictive control with learning (SMPCL) combining the learning of a Markov chain that represents the driver behavior and a scenario-based approach for stochastic optimization. Ref. [22] presented an integrated model predictive control (IMPC) method that combined power management and adaptive velocity control during vehicle-following scenarios in reality, in order to synergistically examine driving safety and fuel economy during vehicle following scenarios of plug-in hybrid electric vehicles (PHEVs).

In this paper, an MPC method based coordinated scheduling optimization for MES is proposed, in which the stochastic nature of EV availability respectively in office or residential sites is investigated considering people's driving patterns, and, moreover, the coordination of two kinds of complementary CHPs is achieved in satisfying the electricity and thermal demands. The main contribution of this paper can be summarized into the following aspects: (1) The uncertain EVs available charging/discharging electricity energy, respectively, in offices and residential buildings is described considering peoples' daily driving pattern, and represented by a number of scenarios generated by scenario generation and reduction techniques; (2) A stochastic MPC approach based electricity-heat coupled MES coordinated scheduling is developed, aiming to achieve the most economic operation in terms of operational costs and EV batteries' degradation costs, while considering operational constraints of various CHPs with complementary properties, which is formulated by a mixed-integer linear programming (MILP) problem and solved by the mature software Cplex. (3) For office or residential buildings, the working modes of EVs are analyzed and discussed; moreover, the energy generation efficiencies of two kinds of CHPs with fixed and variable heat-to-electricity ratio are analyzed.

The rest of this paper is organized as follows: in Section 2, MES structures are introduced, including the system architecture and the components of EVs and CHPs. Section 3 illustrates the stochastic MPC approach for optimal scheduling coordination of MES, including the model and the solving procedure. In Section 4, the simulation results and discussions are described, and two cases are studied to demonstrate the proposed approach. Finally, the paper is concluded in Section 5.

2. Multi-Energy System Structure

MES includes electrical loads, thermal loads, controllable EVs, CHPs, energy storage devices, distributed renewable energy, and the associated electricity, heating and information transmission networks. A typical MES structure is shown in Figure 1. The MES can operate in islanded mode or grid-connected mode by connecting with the external main grid.

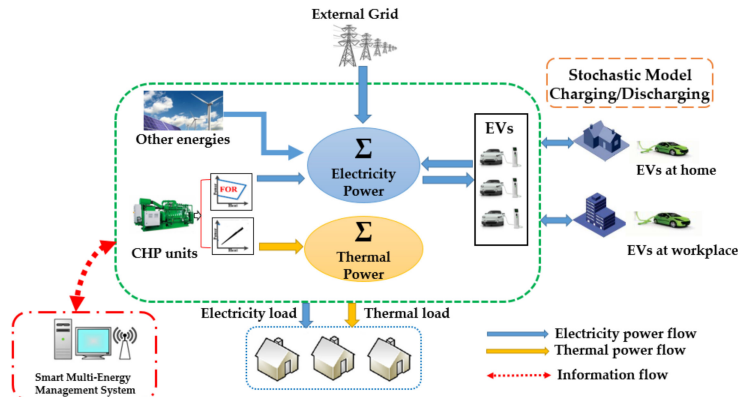


Figure 1. System architecture of a typical multi-energy system (MES). EVs: electric vehicles; CHP: combined heat and power.

The increasing inclusion of plug-in EV has the potential of not only bringing benefits by reducing the on-peak demand, but also improving the economic efficiency. Consequently, in the MES, the scheduling of aggregated EVs is being promoted by persuading the EV owners to participate in the scheduling program. On one hand, the aggregated EVs can be considered as a battery energy storage device in MES when an electricity power imbalance arises or when the buying electricity price from main grid is relatively higher; on the other hand, the aggregated EVs can be regarded as a bulk electricity demand to be charged when the electricity price is cheaper or the load is lower. Consequently, the coordination between EVs and other energy generators in MES has been receiving increasing attention from the researchers. However, there exists an intractable challenge, i.e., the flexibility of available EV charging or discharging electric power and capacity is uncertain and depends on the peoples' daily commuting behaviors, for example when to arrive in the office and when to go home.

As an important energy coupling component, CHP units can supply both electrical and thermal power and can impose significant impacts on the operation of MES. The gas turbine CHP consists mainly of an air compressor, a gas combustion chamber, a turbine, a control system and related auxiliary equipment. The CHP units are classified as backpressure and extraction-condensing units. As shown in Figure 2, the produced thermal power of the back-pressure units depends linearly on the output of the electricity power, thus leading to a limited operation flexibility. For the extraction-condensing units, the operation region in Figure 3 is described as an irregular quadrilateral [23]. Obviously, the feasible operation region (FOR) of the extraction-condensing units is much bigger than that of the backpressure units [24]. The effective coordination between these two types of complementary CHPs makes it possible to simultaneously satisfy electricity and heat demands. In addition, electric heater and heat storage are also installed in MES, in order to offer more flexibility.

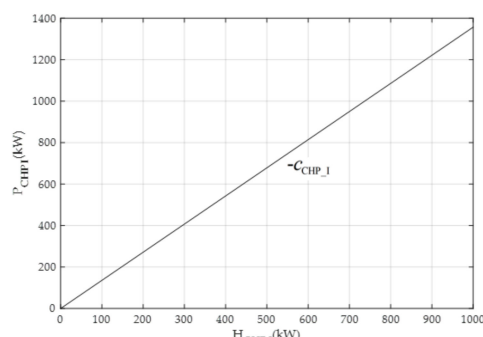


Figure 2. Relationship between thermal and electricity power generation of combined heat and power (CHP) units with fixed heat-to-electricity ratio.

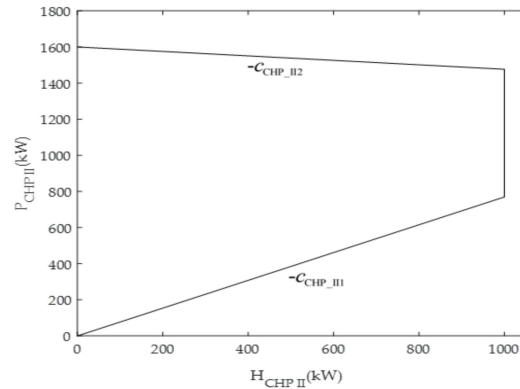


Figure 3. Feasible operation region of CHP unit with variable heat-to-electricity ratio.

The electricity utility company makes a direction guide for charging time of EVs owners by setting peak and valley electricity price for 24 h in a day. The price of natural gas is usually fixed during the period of a day.

3. Stochastic MPC Approach for Coordinated Scheduling Optimization of MES

The studied MES operates in main grid connected mode. In the MES, two types of CHPs with complementary properties are considered, and the EVs are aggregated to be controlled as an electricity load or an electricity supplier. The electricity demands in the MES are satisfied by the main grid, CHPs and EVs; and the thermal demands are provided by two kinds of CHP units. The objective of coordinated scheduling optimization is to achieve the most economic operation while satisfying electricity and thermal power supply/demand balance, the operational constraints of CHP units and EVs.

The stochastic MPC based scheduling optimization of MES, considering the coordination of electricity and heat supplies, is formulated into an MILP problem. The optimization process is composed of two steps. In the first step, the stochastic model of EVs availability is established by using scenario generation and reduction; and, in the second step, the MILP problem is solved, in which minimizing the operation cost is considered as the objective, while considering the supply and demand balance of electricity and heat power and other operational constraints. The schematic overview of the stochastic MPC approach for MES coordinated scheduling optimization is depicted in Figure 4.

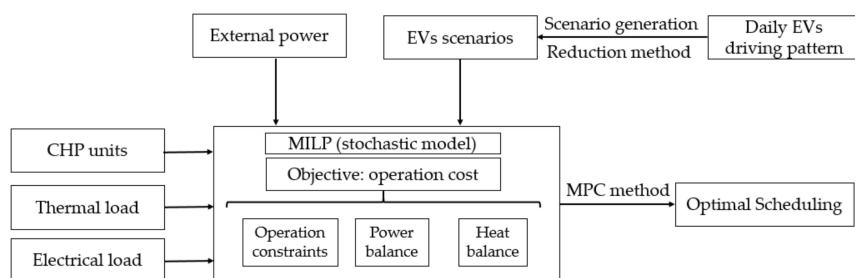


Figure 4. Schematic overview of the stochastic model predictive control (MPC) approach for MES scheduling optimization. MILP: mixed-integer linear programming.

3.1. Modelling of Electric Vehicles' Stochastic Availability

It is assumed that the EV owners immediately connect their EVs to the charging/discharging station in the office or residential building in the morning when they arrive at work and in the evening when they arrive home. In office buildings or residential communities, EV characteristics, in terms of available charging/discharging energy, are quite unique and distinctive, closely depending on peoples' commuting behaviors. In addition, it is worthwhile to note that the availability

of EV charging/discharging is quite uncertain, considering the stochastic individual arrival and departure time.

According to the study which uses driving pattern data of a large number of customers from the National Household Travel Survey (NHTS) [25], the probability distribution of arrival time to the office or home and departure time from the office or home is developed. The arrival/departure time can be represented by a normal distribution and its probability density function (PDF) is described as

$$f(t, \mu, \sigma) = \frac{1}{\sigma\sqrt{2\pi}} \exp\left[-\frac{(t-\mu)^2}{2\sigma^2}\right], 0 < t \leq 24, \quad (1)$$

where f is the probability of arrival/departure time, and μ and σ are its mean value and standard deviation, respectively.

Take the office arrival time as an example to illustrate this. It is assumed that, in the researched office building, the number of EVs participating in scheduling management is NEV . For all the EVs, their arrival times are uncertain variables. Usually, sampling is implemented to generate representative samples, aimed to reflect the distribution of each random variable. For an EV i , the uncertainty of its office arrival time is represented by NS scenarios generated by a Latin Hypercube Sampling (LHS) method considering PDF described in Equation (1) [26]. It is assumed that the arrival events of EVs are independent from each other, i.e., the random variable f_i for EV i is independent from $f_j, j \neq i$. In order to minimize the undesired correlations between the generated samples of different random variables, a permutation method is needed. Cholesky decomposition is a good permutation method, which is helpful for reducing the correlation among the samples of different random variables and can also further improve the performance of LHS. Then, NS scenarios of NEV random variables

$\left\{ \begin{array}{cccc} f_1^1 & \cdots & f_{NEV}^1 \\ \vdots & \ddots & \vdots \\ f_1^{NS} & \cdots & f_{NEV}^{NS} \end{array} \right\}$ are derived. For scenario $s \{f_1^s, \dots, f_{NEV}^s\}$, the available state $I_j^s(t)$ of EV j at time t is defined as $I_j^s(t) = 1, if t \geq round(f_j^s); I_j^s(t) = 0, else$. The available EV number $AN^s(t)$ at time t can be calculated by $AN^s(t) = \sum_j I_j^s(t)$.

NS scenarios of random vector $\{AN^s(1), \dots, AN^s(T)\}, s = 1, \dots, NS$ can be generated using the aforementioned procedure. However, it is time consuming to solve the stochastic scheduling optimization using NS scenarios. The very large set of scenarios has to be approximated by a small number of scenarios using a scenario reduction technique. Here, the backward method is subsequently applied to make the reduced set of scenarios be as close as possible to the original stochastic process.

The probability of each scenario in NS scenarios is $p_s = 1/NS$, and $\sum p_s = 1$. The scenarios set is $\xi_s = \{AN^s(1), \dots, AN^s(T)\}, s = 1, \dots, NS$. The set S and DS represents all scenarios before and after reduction, respectively. Calculating all the distances of a couple of scenarios $DT_{s,s'} = DT(\xi_s, \xi_{s'})$. For the scenario k , the nearest one is r , and calculates the minimum distance of (k, r) scenario couples, $DT_k(r) = \min DT_{k,s'}$. After that, $PD_k(r)$ should be characterized by $PD_k(r) = p_k DT_k(r)$, and find the nearest scenario d , $PD_d = \min PD_k$. Then, the extra scenarios are removed by repeating the above steps, and DS is the reduced scenarios set with DNS scenarios [27].

Step (1) In the first calculation, the DS set is initially empty, the following equation to determine the distance of all couples of scenarios should be applied:

$$DT_{s,s'} = DT(\xi_s, \xi_{s'}) = \sqrt{\sum_{i=1}^d (x_i^s - x_i^{s'})^2}, s, s' \in S. \quad (2)$$

Step (2) For each scenario k , find the minimum distance between scenario r and k by the following equation:

$$DT_k(r) = \min DT_{k,s'}, k, s' \in S, s' \neq r. \quad (3)$$

Step (3) The distance of probability distribution PD_k and PD_d should be characterized by Equations (4) and (5), respectively, and find the nearest scenario d :

$$PD_k(r) = p_k * DT_k(r), k \in S, \quad (4)$$

$$PD_d = \min PD_k, k \in S. \quad (5)$$

Step (4) New scenarios set are generated by the following:

$$S = S - \{d\}, DS = DS + \{d\}, p_r = p_r + p_d. \quad (6)$$

Step (5) Return to Step (2) and repeat; then, the reduced scenario set will be obtained.

The flowchart of a scenario reduction method is shown in Figure 5. The distance of probability distribution is used to be the standard for scenario reduction. The suitable scenario number is determined by balancing the computational burden and scheduling optimization accuracy. The reduced scenarios of available EV number are denoted by $\{DAN^s(1), \dots, DAN^s(T)\}, s = 1, \dots, DNS$ [27,28].

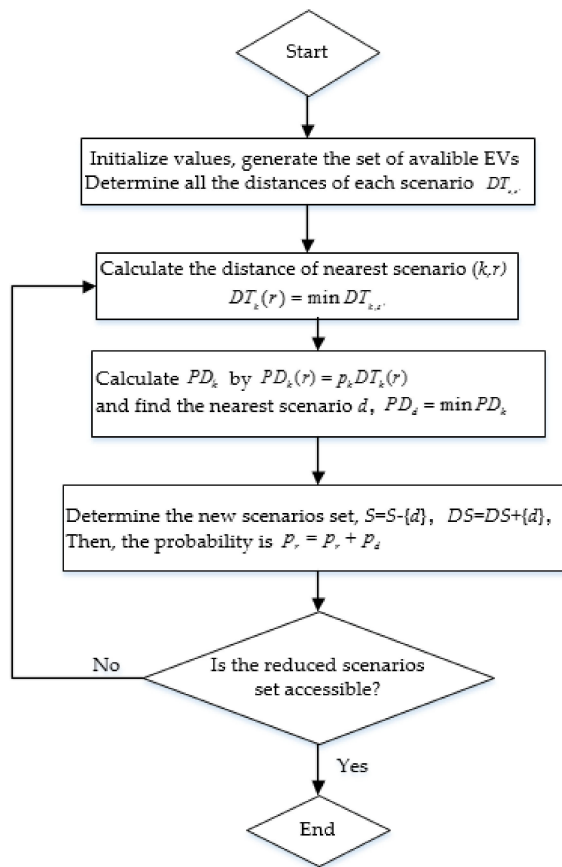


Figure 5. The flow chart of scenario reduction.

3.2. Modelling of Combined Heat and Power Units

The first type of CHP uses a gas turbine or internal combustion reciprocating engine with a fixed heat-electricity ratio, which can be modeled as

$$H_{CHP_I}(t) = c_{CHP_I} P_{CHP_I}(t) \quad (7)$$

$$F_{\text{CHP_I}}(t) = a_{\text{CHP_I}} P_{\text{CHP_I}}(t), \quad (8)$$

where the parameters $c_{\text{CHP_I}}$ and $a_{\text{CHP_I}}$ are considered constant, $H_{\text{CHP_I}}(t)$ and $P_{\text{CHP_I}}(t)$ are the generated heat and electricity power, and $F_{\text{CHP_I}}(t)$ is the power of the consumed natural gas.

The generated electricity power is constrained by

$$0 \leq P_{\text{CHP_I}}(t) \leq P_{\text{CHP_I}}^{\max}. \quad (9)$$

The second type of CHP unit uses extraction steam turbines that can be operated within a wide range of heat-to-electricity ratio. In Equations (10)–(12), the feasible operation region of the CHP is described by a polygon via four lines as shown in Figure 3, where the lines with the slope $c_{\text{CHP_II1}}$ and $-c_{\text{CHP_II2}}$ ($c_{\text{CHP_II2}} > 0$), respectively, define the lower and the upper limits of electric power output with respect to any level of heat power output [28–30]. For the electricity power generation $P_{\text{CHP_II}}(t)$ and the by-product heat power generation $H_{\text{CHP_II}}(t)$, the power of the consumed natural gas by CHP unit is computed in Equation (12):

$$0 \leq H_{\text{CHP_II}}(t) \leq H_{\text{CHP_II}}^{\max}, \quad (10)$$

$$c_{\text{CHP_II1}} H_{\text{CHP_II}}(t) \leq P_{\text{CHP_II}}(t) \leq P_{\text{CHP_II}}^{\max} - c_{\text{CHP_II2}} H_{\text{CHP_II}}(t), \quad (11)$$

$$F_{\text{CHP_II}}(t) = a_{\text{CHP_II}} H_{\text{CHP_II}}(t) + b_{\text{CHP_II}} P_{\text{CHP_II}}(t) + g_{\text{CHP_II}}. \quad (12)$$

The natural gas consumption (m3) by the two CHP units is described as

$$V(t) = (F_{\text{CHP_I}}(t) + F_{\text{CHP_II}}(t)) / \eta, \quad (13)$$

where η (kWh/m3) is the lower heating value of natural gas.

3.3. Model of MPC Based Optimal Scheduling

MPC strategies are quite appealing for energy scheduling of MES, since they allow for the implementation of control actions that anticipate future events such as variations of EVs availability, heat demand and electricity demand. The MPC rolling optimization method usually involves three time sequences: scheduling time sequence, predicting time sequence and controlling time sequence, which is based on iterative, finite-horizon optimization of the controlled model. The rolling optimization method guarantees the optimization of real-time control action by sampling and calculating online [20].

Two 0–1 binary variables B_{ch} and B_{disch} and two continuous variables $X_{\text{ch}} (0 \leq X_{\text{ch}} \leq 1)$ and $X_{\text{disch}} (0 \leq X_{\text{disch}} \leq 1)$ are introduced for describing the SOC and charging/discharging power of the aggregated EVs' batteries. The charging/discharging power and SOC of EVs are modelled as follows:

$$P_{\text{EVs}}^s(t+i|t) = -X_{\text{ch}}^s(t+i|t)DAN^s(t+i)P_{\text{EV_max}} + X_{\text{disch}}^s(t+i|t)DAN^s(t+i)P_{\text{EV_max}}, i = 1, \dots, T, \quad (14)$$

$$X_{\text{ch}}^s(t+i|t) \leq B_{\text{ch}}^s(t+i|t), i = 1, \dots, T, \quad (15)$$

$$X_{\text{disch}}^s(t+i|t) \leq B_{\text{disch}}^s(t+i|t), i = 1, \dots, T, \quad (16)$$

$$B_{\text{ch}}^s(t+i|t) + B_{\text{disch}}^s(t+i|t) \leq 1, i = 1, \dots, T, \quad (17)$$

$$SOC^s(t+i|t) = SOC^s(t+i-1|t) + X_{\text{ch}}^s(t+i|t)P_{\text{EV_max}}\eta_{\text{ch}}/Cap_{\text{EV}} + X_{\text{disch}}^s(t+i|t)P_{\text{EV_max}}/Cap_{\text{EV}}/\eta_{\text{disch}}, i = 1, \dots, T. \quad (18)$$

$P_{\text{EVs}}^s(t+i|t)$ is i -step-ahead dispatched discharging ($P_{\text{EVs}}^s(t+i|t) > 0$)/charging ($P_{\text{EVs}}^s(t+i|t) < 0$) power of the aggregated EVs. $SOC^s(t+i|t)$ is i -step-ahead dispatched state of charge of aggregated EVs, $P_{\text{EV_max}}$ is the maximum charging/discharging power of a EV, Cap_{EV} is the capacity of a EV

battery in kWh, and η_{ch} and η_{disch} are charging and discharging efficiency of EV.

The SOC is limited by its upper and lower boundaries

$$SOC_{\min} \leq SOC^s(t+i|t) \leq SOC_{\max}, i = 0, \dots, T-1. \quad (19)$$

Operational cost can be employed as one of the main objective functions in MES scheduling. The purpose of MES scheduling optimization is to determine the amount of energy generated by the controlled units in the presence of uncontrolled units in a way that the operational cost is minimized while complying with the various operational constraints [30,31]. The optimization objective is to minimize the expected value of the total operating cost during the predictive horizon:

$$\min \sum_s p_s \sum_{i=1}^T c_{\text{Grid}}(t+i|t) P_{\text{Grid}}^s(t+i|t) + c_{\text{Gas}} V(t+i|t) + C_{\text{AEVs}}^s L_{\text{loss}}^s(t+i|t), \quad (20)$$

where T denotes the length of prediction horizon, i is the index of time step in the prediction horizon with $i = 0$ being the current time, $P_{\text{Grid}}^s(t+i|t)$ is i -step-ahead scheduled electricity power exchange between the MES and the external grid, $c_{\text{Grid}}(t+i|t)$ is the i -step-ahead predictive price of exchanged electricity, c_{Gas} is the cost of natural gas, $V(t+i|t)$ is the i -step-ahead scheduled value of natural gas consumption, C_{AEVs}^s is the initial investment cost of the available EVs in scenario s , $L_{\text{loss}}^s(t+i|t)$ is the EVs' batteries life loss proportion of total investment cost, and p_s is the probability of scenario s after scenarios reduction.

The service life of EVs' batteries usually degrades when subjected to repeated charge/discharge cycles. Usually, the battery manufacturers report the relationship between capacity degradation and the number charge/discharge cycle with the fixed operating strategy employed, i.e., the charge/discharge is complete or half cycle. When EVs' batteries are scheduled in practical application, the real charging/discharging process is complicated, representing local cycle, non-complete or complete charging, and so on. Consequently, when considering the degradation cost of EVs' batteries in the optimization objective, the batteries' life loss cost, approximated in the last item on the right side of Equation (20), is included. Usually for an EV's battery, the total cumulative charging/discharging Ah throughput during the whole life cycle can be obtained by manufacturers, denoted by A_{total} . The actual cumulative Ah throughput in a certain period of time is employed to measure the life loss cost of batteries, and then it can be expressed as [32–37]

$$L_{\text{loss}}^s(t+i|t) = \frac{(X_{\text{ch}}^s(t+i|t)P_{\text{EV}-\text{max}} + X_{\text{disch}}^s(t+i|t)P_{\text{EV}-\text{max}}) \cdot \Delta t}{A_{\text{total}}}. \quad (21)$$

The initial investment cost C_{AEVs}^s can be defined as

$$C_{\text{AEVs}}^s = C_p D_{\text{AN}}^s(t+i) P_{\text{EV}-\text{max}} + C_c D_{\text{AN}}^s(t+i) C_{\text{ap}}_{\text{EV}}. \quad (22)$$

In addition to the operation constraints of CHP units and EVs represented in Equations (7)–(19), the supply and demand balance of electricity and thermal energy are considered as follows:

(1) Electricity power supply and demand balance

The electricity supply and demand balance should be imposed, which is described as follows:

$$P_{\text{EVs}}^s(t+i|t) + P_{\text{CHP_I}}(t+i|t) + P_{\text{CHP_II}}(t+i|t) + P_{\text{Grid}}^s(t+i|t) = P_{\text{load}}(t+i|t), i = 1, \dots, T, \quad (23)$$

where $P_{\text{CHP_I}}(t+i|t)$ and $P_{\text{CHP_II}}(t+i|t)$ are i -step-ahead scheduled values of CHP electricity power generation, and $P_{\text{load}}(t+i|t)$ is the electricity demand.

Power exchange between the MES and the external main grid is constrained by

$$0 \leq P_{\text{Grid}}^s(t+i|t) \leq P_{\text{Grid}}^{\max}, \quad (24)$$

where P_{Grid}^{\max} is the maximum power purchasing from external grid.

(2) Thermal power supply and demand balance

Practically, it is not necessary that the thermal supply is absolutely balanced by its demand; on the contrary, maintaining the thermal supply and demand balance within an accepted range is desirable. Consequently, the thermal supply and demand balance should follow the following constraints:

$$\eta_{h1} H_{\text{load}}(t+i|t) \leq H_{\text{CHP_I}}(t+i|t) + H_{\text{CHP_II}}(t+i|t) \leq \eta_{h2} H_{\text{load}}(t+i|t), i = 1, \dots, T, \quad (25)$$

where η_{h1} and η_{h2} are the lower and upper allowed fluctuation coefficients.

3.4. Solving Procedure of MPC Based Optimal Scheduling

In the proposed MPC method, the solution to the optimal control problem of MES is solved over a certain pre-defined horizon using the current state of the system as the initial state at each time step. The optimization calculates a control sequence for the whole horizon such that the selected objectives are minimized, but only the control action for the next time step is implemented; the horizon is shifted forward and the process is then repeated at the next time step [21]. A finite-horizon optimal control problem is solved repeatedly, the procedure of which is illustrated by Figure 6. In this simulation, the prediction horizon of MPC is chosen as $T = 4$. Firstly, the MPC controller will calculate the scheduling results over four time periods at the current time constant. Then, a four-dimensional optimal controller can be obtained; however, only the first component of this solution will be actually executed at this time instant. Finally, the optimization horizon will move one step forward, and the optimization will be repeated on the next interval of four time periods with the updated initial values.

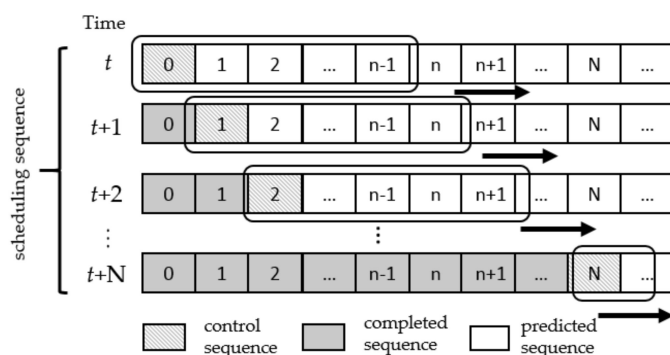


Figure 6. Explanation of time sequences in rolling optimization of MPC.

The procedure of applying the proposed stochastic MPC algorithm in the operation optimization of MES is illustrated as follows:

- Step (1) When $t = 0$, obtain the reduced scenarios of available EV number at each hour by LHS and scenario reduction techniques, and initialize the parameters.
- Step (2) Solve the stochastic MPC optimization model over the following prediction time horizon T , i.e., the objective (20) and the constraints Equations (7)–(19) and Equations (21)–(25), with respect to time t via Cplex.
- Step (3) The prediction time horizon is shifted forward (i.e., the time instant moves to $t = t + 1$) and implement the first control action, i.e., the scheduled results of $P_{\text{CHP_I}}(t+1|t)$,

$P_{\text{CHP_II}}(t + 1|t)$ and the expected value of the aggregated EVs power on the system.

Step (4) Update the initial parameters, return to Step (2) and repeat.

In the proposed approach, the short-term-ahead scheduling of MES is formulated as an MPC problem. During the considered prediction horizon, the optimization objective is to minimize the total operational cost, the constraints for the power supply/demand balance are applied, and the bounds for charging/discharging power of EVs are imposed for a total number of scenarios of uncertain EVs' model. With the MPC approach considering the scenario optimization, the operational cost can be minimized while the supply and demand balance of electricity and heat is achieved by coordinating the supply of CHPs and uncertain available EVs properly.

4. Simulation Results and Discussion

The proposed scheduling optimization approach is implemented in the MES, which is connected to the external main grid, considering EV charging/discharging, battery degradation, two types of complementary CHPs, thermal load and electrical load for a 24-h period. The stochastics of EVs owners' arrival and departure times respectively for office and residential buildings are modelled. LHS scenarios generation and backward scenarios reduction method is used to generate the suitable number of scenarios of EVs available charging/discharging in two cases of office and residential buildings. The Time of Use (TOU) pricing for electricity consumption and the fixed price for natural gas are utilized in optimal economic dispatch [38]. The proposed MPC optimization approach considering scenarios can be formulated to be a mixed inter linear programming (MILP) problem, which can be solved by the commercial software Cplex. Considering the EVs owners' commuting behavior, two cases were investigated in this paper [12,39,40]:

Case 1: MES in office building.

Case 2: MES in residential building.

4.1. Case 1: MES in Office Buildings

A typical day is chosen to support the details of the research, the period of MPC based scheduling is 24 h and Δt is 1 h. The office arrival time of EVs owners is represented by a normal distribution with mean value 9:00 a.m. and standard deviation 1 h; and the office departure time follows a normal distribution with mean value 6:00 p.m. and standard deviation 1 h. The scenarios of the available number of EVs at each time are generated by scenarios generation and reduction technique. It is assumed that the thermal power demand is completely dependent on the CHP units without additional equipment [41,42]. The capacity of each EV is assumed to be 48 kWh, and the total number of available EVs is 100 in this case. The lower and upper limits of aggregated SOC are set to be 0.3 and 1. The TOU pricing for electricity consumption and the fixed price for natural gas are shown in Table 1, in which four different electricity prices during a day are considered.

Table 1. Energy tariff in Case 1.

Item	Valley (00:00 a.m.–7:00 a.m.)	Flat (8:00 a.m.–10:00 a.m., 7:00 p.m.–11:00 p.m.)	Peak (11:00 a.m.–12:00 a.m., 4:00 p.m.–6:00 p.m.)	High Peak (1:00 p.m.–3:00 p.m.)
Electricity from main grid	0.3539 RMB/kWh	0.7785 RMB/kWh	1.2283 RMB/kWh	1.3377 RMB/kWh
Price of Gas	Case 1 3.4 RMB/m ³			

Two thousand scenarios are generated by using the LHS method and the number of scenarios is further reduced to 10 by using the scenario reduction technique. The reduced scenarios $\{DAN^s(1), \dots, DAN^s(T)\}, s = 1, \dots, 10$ are depicted in Figure 7 and the probabilities of the reduced

scenarios are given in Table 2, the sum of which is equal to 1. It is discovered from Figure 7 that most of the EVs arrive in office buildings at 9:00 am., and most of the EVs' owners get off work when $t = 6:00$ p.m.

Table 2. The probabilities of reduced scenarios in Case 1.

Scenarios	s1	s2	s3	s4	s5	s6	s7	s8	s9	s10
probabilities	0.075	0.060	0.151	0.075	0.110	0.089	0.082	0.142	0.060	0.156

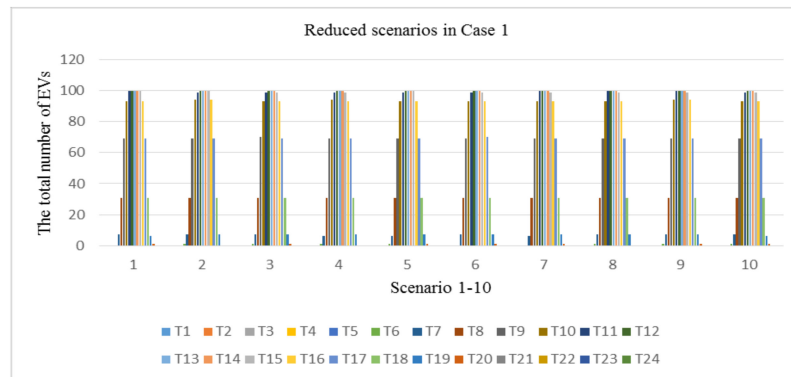


Figure 7. The reduced scenarios of total number of available EVs at each time instant in Case 1.

The electrical and thermal demands during 24 h are depicted in Figure 8a, b respectively. When it is 8:00 a.m., the electricity demand begins to increase; during 12:00 p.m.–1:00 p.m. have a slight drop, and after 6:00 p.m., the demand begins to fall steadily. The thermal demand is higher during the time period 9:00 a.m.–6:00 p.m.

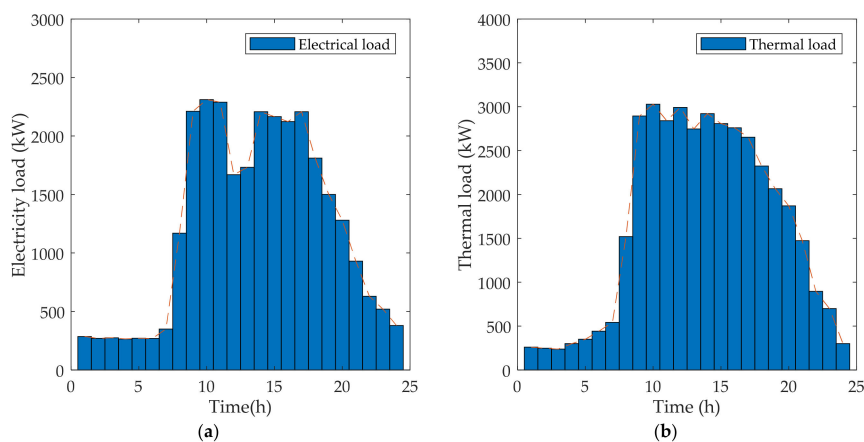


Figure 8. Energy consumption load in Case 1: (a) electrical load, (b) thermal load.

The electricity and thermal scheduling results are shown in Figures 9–11. The aggregated SOC of EVs is drawn in Figure 12. During the period 8:00 a.m.–12:00 a.m. and 1:00 p.m.–6:00 p.m., with the relatively higher electricity price and more available EVs, there is no electricity purchasing from the connected main grid, and the thermal and electric demands are satisfied by the CHP units and EVs. Even during the period 12:00 a.m.–1:00 p.m., the electricity generations from CHP units can not only provide all the electric demand, but also charge the EVs, making its aggregated SOC rise a little during the steady descending process shown in Figure 12. No purchasing electricity power from extern main grid during the period of higher price shows an expected economic efficiency. During the period 9:00 a.m.–8:00 p.m. when the electricity and thermal demands are higher, as CHP_I with a fixed heat-to-electricity ratio has a higher energy conversion efficiency compared with CHP_II,

it works at full-load state and then the gap between the thermal demand and the CHP_I heat generation is provided by CHP_II, indicating the coordinated optimization.

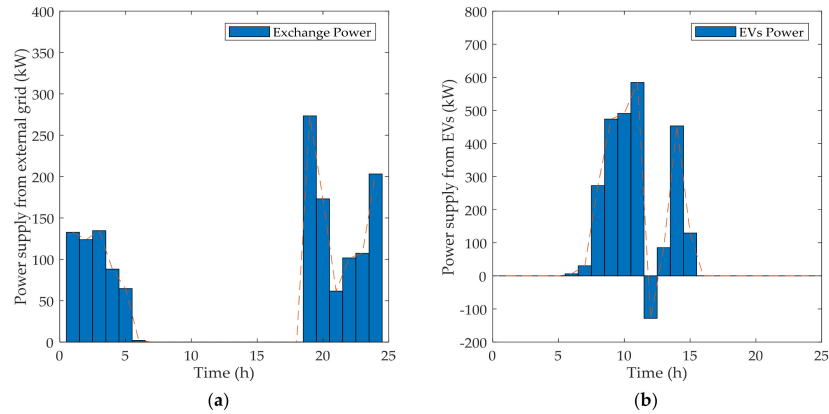


Figure 9. Electrical power supply in Case 1: (a) from the external grid and (b) from EVs.

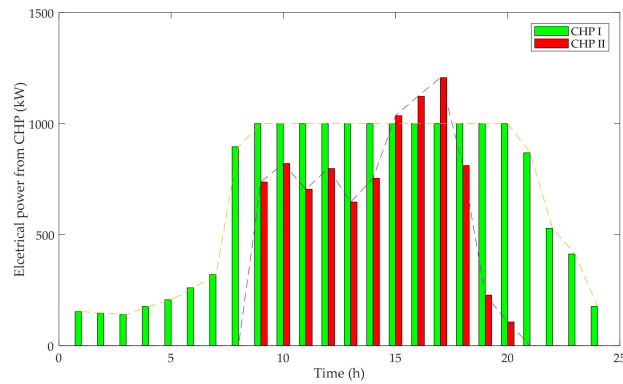


Figure 10. Electrical power supply from CHP_I and CHP_II in Case 1.

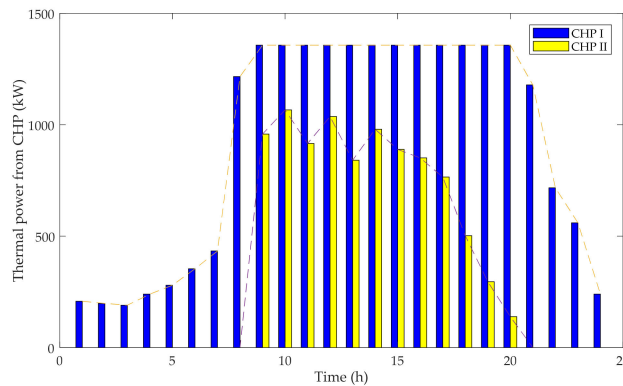
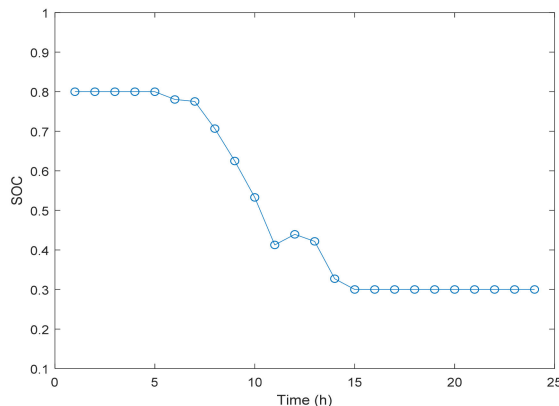


Figure 11. Thermal power supply from CHP_I and CHP_II in Case 1.

**Figure 12.** Aggregated SOC of EVs in Case 1.

4.2. Case 2: MES in Residential Building

In this case, the home arrival time of EVs owners in the evening is also described by a normal distribution with mean value 7:00 p.m. and standard deviation 1 h; and the home departure time in the morning follows a normal distribution with mean value 8:00 a.m. and standard deviation 1 h. The stochastic characteristics of EVs are represented by the reduced scenarios of the available number of the aggregated EVs at each time [43,44]. The capacity of each EV is assumed to be 20 kWh, and the total number of aggregated EVs is 100 in this case. The upper limit of SOC is set to be 1. The lower limit of SOC is set to be 0.3 during 10:00 a.m.–10:00 p.m., 0.5 during 11:00 p.m.–4:00 a.m., and 0.8 during 5:00 a.m.–9:00 a.m. considering the schedulability of EVs induced by the peak/valley price and departure time. The energy tariff is shown in Table 3.

Table 3. Energy tariff in Case 2.

Price of Electricity	Valley (1:00 a.m.–7:00 a.m., 11:00 p.m.–12:00 p.m.)		Peak (8:00 a.m.–10:00 p.m.)
	0.288 RMB/kWh	0.668 RMB/kWh	
Price of Gas	Case 2 3.4 RMB/m ³		

Similarly, two thousand scenarios are generated by using the LHS method and the number of scenarios is further reduced to 10 by using the scenario reduction technique. The probabilities of the reduced scenarios are given in Table 4; as is shown, the sum of scenario probability is also equal to 1. The total available EV number at each time instant for the reduced scenarios in Case 2 is depicted in Figure 13. Compared with Figure 7, it is shown that, in the residential building, the total number of available EVs begins to increase when off work and most of the EVs are available during the period 8:00 p.m.–6:00 a.m.

Table 4. The probabilities of reduced scenarios in Case 2.

Scenarios	s1	s2	s3	s4	s5	s6	s7	s8	s9	s10
probabilities	0.075	0.151	0.134	0.110	0.089	0.082	0.143	0.073	0.060	0.083

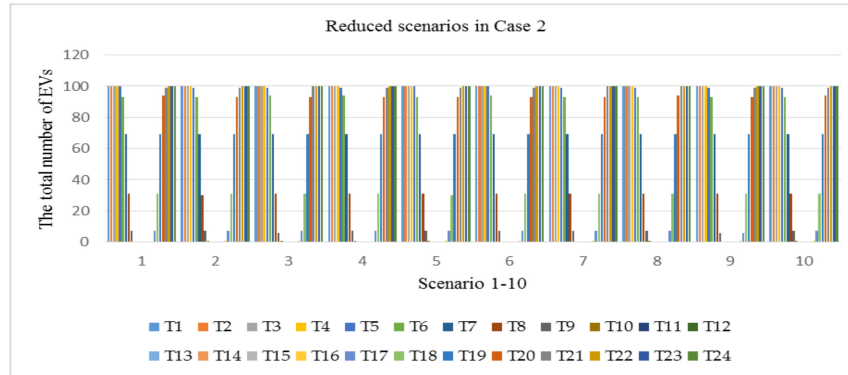


Figure 13. The number of available EVs for reduced scenarios in Case 2.

In Figure 14, the electrical and thermal loads in residential building are drawn. It is obvious that, during the time periods 7:00 a.m.–9:00 a.m. and 5:00 p.m.–10:00 p.m., the electricity and thermal demands are relatively higher, and the average value of period 5:00 p.m.–10:00 p.m. is much higher than that of 7:00 a.m.–9:00 a.m. The profile of electricity and thermal demands is in accordance with the peoples' living habits.

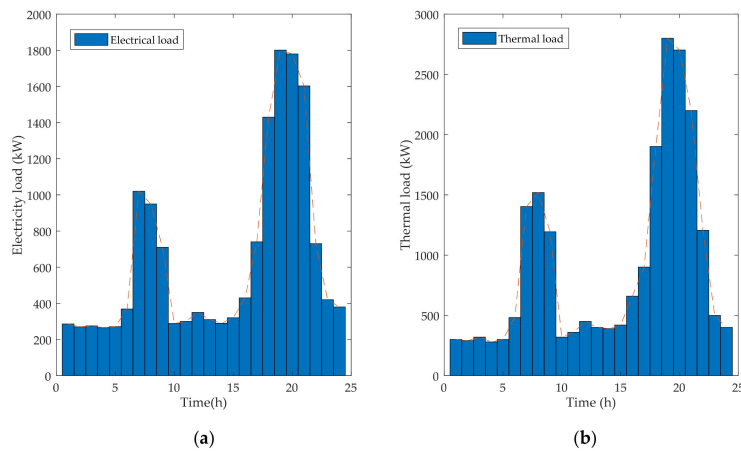


Figure 14. Energy consumption load in Case 2: (a) electrical load, (b) thermal load.

The scheduling results of the aggregated EVs, the external main grid and two kinds of CHP units are depicted in Figures 15–17. The aggregated SOC of EVs is depicted in Figure 18. During the time period 5:00 p.m.–10:00 p.m., with the increase of available EVs and the higher electricity price, EVs are scheduled to serve as an electricity energy supplier by discharging to help satisfy the higher electricity demand; and, even during the period 6:00 p.m.–10:00 p.m. when the thermal and electricity demands stay at a peak level, no purchasing electricity from the external main grid can be achieved. The charging of EVs is scheduled at the valley periods 0:00 a.m.–1:00 a.m. and 4:00 a.m.–5:00 a.m. As shown in Figures 16 and 17, since the electrical and thermal demand is lower except the period 6:00 p.m.–9:00 p.m., only the coordination of CHP_I unit and the connected main grid can satisfy the multi-energy demands during 10:00 p.m.–5:00 p.m., with the CHP_II unit being off; during the period 6:00 p.m.–9:00 p.m., with the higher energy demands, CHP_II units are scheduled to provide the multi-energy, together with the external main grid and CHP_I unit working at full-load state. The coordinated scheduling of the different kinds of CHP units can indicate the fact that the CHP_I unit has a higher energy conversion efficiency, and the lower operating costs. All such scheduling results can achieve a desired economic optimization.

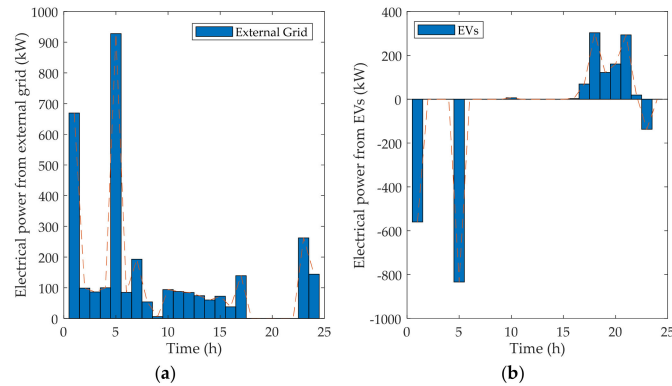


Figure 15. Electrical power supply in Case 2: (a) from the external grid and (b) from EVs.

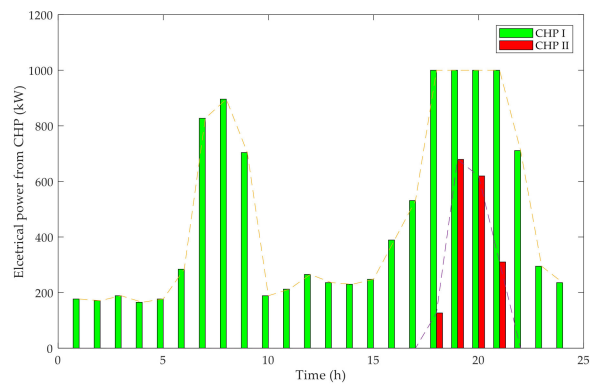


Figure 16. Electrical power supply from CHP_I and CHP_II in Case 2.

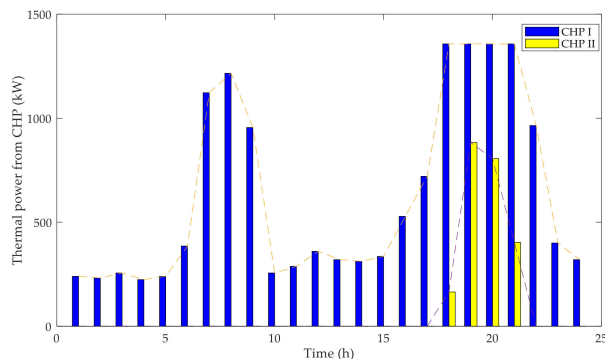


Figure 17. Thermal power supply from CHP_I and CHP_II in Case 2.

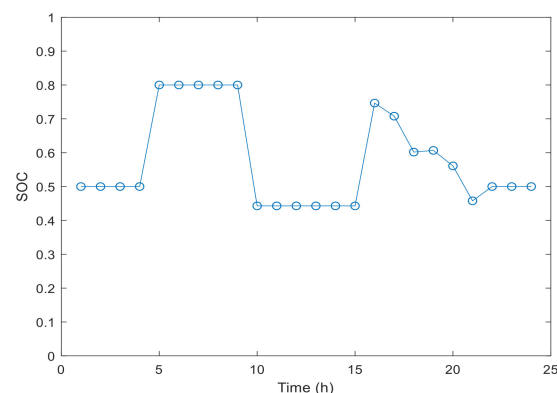


Figure 18. Aggregated value of SOC in Case 2.

4.3. Discussion

This proposed approach is demonstrated by two distinct scenarios, office building and residential building, with the desired scheduling results of various energy generators. The total operational costs in Case 1 and Case 2 are 25223.47 RMB and 13645.52 RMB, respectively. In Case 1, the aggregated EVs are scheduled to discharge to satisfy the electricity demand, along with the CHP units and the connected main grid. In Case 2, the aggregated EVs are dispatched to charge during valley periods and discharge during peak periods. With the effective utilization of TOU electricity pricing and the available aggregated EVs, the economic operation can be effectively achieved by the proposed approach. Take Case 1 as an example to calculate the energy conversion efficiencies of the CHP_I and CHP_II unit, which are $\eta_{CHP_I} = 89.17\%$ and $\eta_{CHP_II} = 61.85\%$, respectively.

As can be seen in Figures 9a and 15a, the general tendency of purchasing electricity power from the external main grid changes is in accordance with the variation of electrical load and electricity price. Comparing Figures 14a and 15a,b, the aggregated EVs are charged at night when the electricity is at a low level price and the power demand is low, and, as a result, more electrical power will be purchased from the main grid. The trend toward higher discharging power ratings can be combined with the peak shaving. In addition, the combination of different facilities is likely to further promote the comprehensive benefit of the MES. A comparison between the experimental data in Figures 9, 10, 15 and 16 shows the tendency of evolutionary processes compatibly, according to the variable electricity price and power consumption. These strategies allow a high number of EVs to be charged or discharged in either office or residential building with a lower impact on the connected main grid and an increased flexible consumption.

5. Conclusions

This paper proposes a stochastic MPC approach to investigate the modeling, coordinated optimal economic scheduling, and analysis of the MES. The stochastic nature of EVs available charging/discharging electric power respectively in offices and residential buildings is investigated considering EVs owners' commuting pattern and represented by a number of scenarios that are generated by LHS and scenario reduction techniques. The charging/discharging degradation cost of EVs batteries is also taken into consideration. Two types of CHP units with complementary properties are applied to supply electrical and thermal energy, considering their different operational characteristics. The stochastic MPC scheme is formulated by a MILP problem, taking the coordinated economic operation as an objective, while considering various operational constraints and uncertain EV availability. The MPC base MES scheduling optimization can be solved by Cplex. The simulations of two representative cases, office and residential building, are conducted to evaluate the proposed approach, in which the TOU pricing of electricity energy purchasing from external main grid and two CHPs with fixed and variable heat-to-electricity ratios are included [45–47]. In office buildings, the aggregated EVs are scheduled to serve as an electricity supplier during the daytime when the electricity price stays at peak level—moreover, CHP units, aggregated EVs and the connected main grid coordinates to satisfy the thermal and electricity demands simultaneously. In residential buildings, the aggregated EVs are scheduled to be charged during the night when the electricity price is lower, and the coordination among several energy suppliers is achieved. The simulations results demonstrate the feasibility and effectiveness of the proposed approach on the multi-energy coordination while considering the uncertainties and battery degradation of EVs.

In future work, the proposed solution can be further improved through incorporating realistic energy systems and using a massive number of field statistics [46–48]. Renewable energy such as wind power and photovoltaic energy will be considered to investigate how intermittency affects the economic goal and the balance of the MES.

Author Contributions: X.G. and Z.B. mainly proposed the approach, designed the simulation, and wrote the paper. Z.B. revised and analyzed the results. W.Y. provided some key issues' improvement strategies to strengthen

the algorithm performance, helped verify the idea and partially wrote the paper. All of the authors worked together to finish the implementation of the whole algorithm and paper writing.

Funding: This work was supported by the National Natural Science Foundation of China under Grant No. 51777182.

Conflicts of Interest: The authors declare no conflict of interest.

References

1. International Energy Agency. *Energy Technology Perspectives 2012: Pathways to a Clean Energy System*; International Energy Agency: Paris, France, 2012.
2. Krause, T.; Andersson, G.; Froehlich, K.; Vaccaro, A. Multiple-energy carriers: Modeling of production, delivery, and consumption. *Proc. IEEE* **2011**, *99*, 15–27. [[CrossRef](#)]
3. Wu, J.; Yan, J.; Jia, H.; Hatziaargyriou, N.; Djilali, N.; Sun, H. Integrated energy systems. *Appl. Energy* **2016**, *167*, 155–157. [[CrossRef](#)]
4. Harighi, T.; Bayindir, R.; Padmanaban, S.; Mihet-Popa, L.; Hossain, E. An Overview of Energy Scenarios, Storage Systems and the Infrastructure for Vehicle-to-Grid Technology. *Energies* **2017**, *10*, 3390. [[CrossRef](#)]
5. Passey, R.; Spooner, T.; MacGill, I.; Watt, M.; Syngellakis, K. The potential impacts of grid-connected distributed generation and how to address them: A review of technical and non-technical factors. *Energy Policy* **2011**, *39*, 6280–6290. [[CrossRef](#)]
6. Sadeghian, H.; Wang, Z. Combined heat and power unit commitment with smart parking lots of plug-in Electric Vehicles. In Proceedings of the North American Power Symposium (NAPS), Morgantown, WV, USA, 17–19 September 2017.
7. Mohammadkhani, N.; Sedighizadeh, M.; Esmaili, M. Energy and emission management of CCHPs with electric and thermal energy storage and electric vehicle. *Therm. Sci. Eng. Prog.* **2018**, *8*, 494–508. [[CrossRef](#)]
8. Farsangi, A.S.; Hadayeghparast, S.; Mehdinejad, M.; Shayanfar, H. A novel stochastic energy management of a microgrid with various types of distributed energy resources in presence of demand response programs. *Energy* **2018**, *160*, 257–274. [[CrossRef](#)]
9. Melhem, F.Y.; Grunder, O.; Hammoudan, Z.; Moubayed, N. Optimization and energy management in smart home considering photovoltaic, wind, and battery storage system with integration of Electric Vehicles. *Can. J. Electr. Comput. Eng.* **2017**, *40*, 128–138.
10. Conejo, A.J.; Carrion, M.; Morales, J.M. *Decision Making Under Uncertainty in Electricity Markets*; Springer: Berlin, Germany, 2010.
11. Liu, H.; Qi, J.; Wang, J.; Li, P.; Li, C.; Wei, H. EV dispatch control for supplementary frequency regulation considering the expectation of EV owners. *IEEE Trans. Smart Grid* **2018**, *9*, 3763–3772. [[CrossRef](#)]
12. Odkhuu, N.; Lee, K.; Ahmed, M.A.; Kim, Y. Optimal energy management of V2B with RES and ESS for peak load minimization. *Appl. Sci.* **2018**, *8*, 2125. [[CrossRef](#)]
13. Huang, Q.; Jia, Q.; Guan, X. Robust scheduling of EV charging load with uncertain wind power integration. *IEEE Trans. Smart Grid* **2018**, *9*, 1043–1054. [[CrossRef](#)]
14. Ju, L.; Li, P.; Tan, Q.; Wang, L.; Tan, Z.; Wang, W.; Qu, J. A multi-objective scheduling optimization model for a multi-energy complementary system considering different operation strategies. *Appl. Sci.* **2018**, *8*, 2293. [[CrossRef](#)]
15. Klayklueng, T.; Dechanupaprittha, S.; Kongthong, P. Analysis of unbalance plug-in Electric Vehicle home charging in PEA distribution network by stochastic load model. In Proceedings of the International Symposium on Smart Electric Distribution Systems and Technologies (EDST), Vienna, Austria, 8–11 September 2015.
16. Cao, J.; Crozier, C.; McCulloch, M.; Fan, Z. Optimal design and operation of a low carbon community based multi-energy systems considering EV integration. *IEEE Trans. Sustain. Energy (Early Access)* **2018**, *6*, 1–9. [[CrossRef](#)]
17. Duan, R.; Ma, Z. Resident Electric Vehicles charging optimization strategy in the smart grid. In Proceedings of the Chinese Control Conference (CCC), Hangzhou, China, 14 September 2015.
18. Shafie-khah, M.; Siano, P. A stochastic home energy management system considering satisfaction cost and response fatigue. *IEEE Trans. Ind. Inform.* **2018**, *14*, 629–638. [[CrossRef](#)]

19. Wu, D.; Zeng, H.; Lu, C.; Boulet, B. Two-stage energy management for office buildings with workplace EV charging and renewable energy. *IEEE Trans. Transp. Electrif.* **2017**, *3*, 225–237. [[CrossRef](#)]
20. Di Cairano, S.; Bernardini, D.; Bemporad, A.; Kolmanovsky, I.V. Stochastic MPC with learning for driver-predictive vehicle control and its application to HEV energy management. *IEEE Trans. Control Syst. Technol.* **2014**, *22*, 1018–1031. [[CrossRef](#)]
21. Guo, X.; Bao, Z.; Li, Z.; Yan, W. Adaptively constrained stochastic model predictive control for the optimal dispatch of microgrid. *Energies* **2018**, *11*, 243. [[CrossRef](#)]
22. Xie, S.; Hu, X.; Liu, T.; Qi, S.; Lang, K.; Li, H. Predictive vehicle-following power management for plug-in hybrid electric vehicles. *Energy* **2018**, *166*, 701–714. [[CrossRef](#)]
23. Christidis, A.; Koch, C.; Pottel, L.; Tsatsaronis, G. The contribution of heat storage to the profitable operation of combined heat and power plants in liberalized electricity markets. *Energy* **2012**, *41*, 75–82. [[CrossRef](#)]
24. Li, P.; Wang, H.; Lv, Q.; Li, W. Combined heat and power dispatch considering heat storage of both buildings and pipelines in district heating system for wind power integration. *Energies* **2017**, *10*, 893. [[CrossRef](#)]
25. U.S. Department of Transportation, Federal Highway Administration. 2009 National Household Travel Survey. Available online: <http://nhts.ornl.gov> (accessed on 18 October 2018).
26. Stein, M. Large sample properties of simulations using Latin Hypercube Sampling. *Technometrics* **1978**, *29*, 143–151. [[CrossRef](#)]
27. Yu, H.; Chung, C.Y.; Wong, K.P.; Lee, H.W.; Zhang, J.H. Probabilistic load flow evaluation with hybrid Latin Hypercube Sampling and Cholesky decomposition. *IEEE Trans. Power Syst.* **2009**, *24*, 661–667. [[CrossRef](#)]
28. Tavakoli, M.; Shokrideraki, F.; Marzband, M.; Godina, R.; Pouresmaeil, E. A two stage hierarchical control approach for the optimal energy management in commercial building microgrids based on local wind power and PEVs. *Sustain. Cities Soc.* **2018**, *41*, 332–340. [[CrossRef](#)]
29. Bornapour, M.; Hooshmand, R.; Khodabakhshian, A.; Parastegari, M. Optimal stochastic scheduling of CHP-PEMFC, WT, PV units and hydrogen storage in reconfigurable micro grids considering reliability enhancement. *Energy Convers. Manag.* **2017**, *150*, 725–741. [[CrossRef](#)]
30. Yuan, R.; Ye, J.; Lei, J.; Li, T. Integrated combined heat and power system dispatch considering electrical and thermal energy storage. *Energies* **2016**, *9*, 474. [[CrossRef](#)]
31. Zhou, F.; Xiao, F.; Chang, C.; Shao, Y.; Song, C. Adaptive model predictive control-based energy management for semi-active hybrid energy storage systems on Electric Vehicles. *Energies* **2017**, *10*, 1063. [[CrossRef](#)]
32. Zhao, B.; Zhang, X.; Chen, J.; Wang, C.; Guo, L. Operation Optimization of Standalone Microgrids Considering Lifetime Characteristics of Battery Energy Storage System. *IEEE Trans. Sustain. Energy* **2013**, *4*, 934–943. [[CrossRef](#)]
33. He, G.; Chen, Q.; Kang, C.; Pinson, P.; Xia, Q. Optimal Bidding Strategy of Battery Storage in Power Markets Considering Performance-Based Regulation and Battery Cycle Life. *IEEE Trans. Smart Grid* **2016**, *7*, 2359–2367. [[CrossRef](#)]
34. Jenkins, D.P.; Fletcher, J.; Kane, D. Lifetime prediction and sizing of lead–acid batteries for microgeneration storage applications. *IET Renew. Power Gener.* **2008**, *2*, 191–200. [[CrossRef](#)]
35. Tazvinga, H.; Zhu, B.; Xia, X. Optimal power flow management for distributed energy resources with batteries. *Energy Convers. Manag.* **2015**, *102*, 104–110. [[CrossRef](#)]
36. Zhou, B.; Liu, X.; Cao, Y.; Li, C.; Chung, C.Y.; Chan, K.W. Optimal scheduling of virtual power plant with battery degradation cost. *IET Gener. Transm. Distrib.* **2016**, *10*, 712–725. [[CrossRef](#)]
37. Duggal, I.; Venkatesh, B. Short-Term Scheduling of Thermal Generators and Battery Storage with Depth of Discharge-Based Cost Model. *IEEE Trans. Power Syst.* **2015**, *30*, 2110–2118. [[CrossRef](#)]
38. Samuel, O.; Javaid, S.; Javaid, N.; Ahmed, S.H.; Khalil, M.; Ishmanov, F. An efficient power scheduling in smart homes using Jaya based optimization with Time-of-Use and critical peak pricing schemes. *Energies* **2018**, *11*, 3155. [[CrossRef](#)]
39. Thomas, D.; Deblecker, O.; Ioakimidis, C.S. Optimal operation of an energy management system for a grid-connected smart building considering photovoltaics' uncertainty and stochastic electric vehicles' driving schedule. *Appl. Energy* **2018**, *210*, 1188–1206. [[CrossRef](#)]
40. Liu, Z.; Chen, Y.; Zhuo, R.; Jia, H. Energy storage capacity optimization for autonomy microgrid considering CHP and EV scheduling. *Appl. Energy* **2018**, *210*, 1113–1125. [[CrossRef](#)]

41. Quddus, M.A.; Shahvari, O.; Marufuzzaman, M.; Usher, J.M.; Jaradat, R. A collaborative energy sharing optimization model among electric vehicle charging stations, commercial buildings, and power grid. *Appl. Energy* **2018**, *229*, 841–857. [[CrossRef](#)]
42. Wang, Y.; Yu, H.; Yong, M.; Huang, Y.; Zhang, F.; Wang, X. Optimal scheduling of integrated energy systems with combined heat and power generation, photovoltaic and energy storage considering battery lifetime loss. *Energies* **2018**, *11*, 1676. [[CrossRef](#)]
43. Barata, F.; Igreja, J. Energy Management in Buildings with Intermittent and Limited Renewable Resources. *Energies* **2018**, *11*, 2748. [[CrossRef](#)]
44. Kitapbayev, Y.; Moriarty, J.; Mancarella, P. Stochastic control and real options valuation of thermal storage-enabled demand response from flexible district energy systems. *Appl. Energy* **2015**, *137*, 823–831. [[CrossRef](#)]
45. Korolko, N.; Sahinoglu, Z. Robust optimization of EV charging schedules in unregulated electricity markets. *IEEE Trans. Smart Grid* **2017**, *8*, 149–157. [[CrossRef](#)]
46. Ma, T.; Wu, J.; Hao, L.; Lee, W.; Yan, H.; Li, D. The optimal structure planning and energy management strategies of smart multi energy systems. *Energy* **2018**, *160*, 122–141. [[CrossRef](#)]
47. Yu, Y.; Chen, H.; Chen, L. Comparative study of electric energy storages and thermal energy auxiliaries for improving wind power integration in the cogeneration system. *Energies* **2018**, *11*, 263. [[CrossRef](#)]
48. Sulaimana, N.; Hannanb, M.A.; Mohamedc, A.; Kerb, P.J.; Majlana, E.H.; Dauda, W.R.W. Optimization of energy management system for fuel-cell hybrid electric vehicles: Issues and recommendations. *Appl. Energy* **2018**, *228*, 2061–2079. [[CrossRef](#)]



© 2019 by the authors. Licensee MDPI, Basel, Switzerland. This article is an open access article distributed under the terms and conditions of the Creative Commons Attribution (CC BY) license (<http://creativecommons.org/licenses/by/4.0/>).